Supporting Material of: Anomalous behavior in the nucleation of ice at negative pressures

Valentino Bianco[1], Pablo Montero de Hijes[1], Cintia P. Lamas[1], Eduardo Sanz[1], Carlos Vega[1]
[1] *Faculty of Chemistry, Chemical Physics Department, Universidad Complutense de Madrid, Plaza de las Ciencias, Ciudad Universitaria, Madrid 28040, Spain**

* vabianco@ucm.es, cvega@ucm.es

DIRECT COEXISTENCE SIMULATIONS

To determine the solid-liquid equilibrium line we place a block of ice Ih consisting of 4032 molecules in contact with an equal number of liquid molecules. We perform NPT simulations, with anisotropic P to relax the crystal structure, counting the number of solid molecules in time. Along an isobar, if T is larger than the coexistence temperature the ice melts, hence the number of solid particles decreases in time. On the other hand, for T below the coexistence temperature the number of solid molecules increases in time. The coexistence T is determined when, for independent trajectories, the ice shows equal probability of melting or growing.

SEEDING SIMULATIONS

The purpose of this technique is to find the critical nucleus size at a certain temperature T and pressure P. Given that the critical nucleus is situated at the top of the energy barrier, it is in unstable equilibrium and the probability for the nucleus to grow or to shrink is equally 50%. Therefore, by inserting a crystal seed of a given size N within the bulk liquid and tracking its evolution with time over multiple independent runs, we can estimate if N is larger than the crytical size N_c (meaning that all the crystal seeds grow) or if it is smaller (in which case all the seeds melt). When $N \sim N_c$ we expect to observe the ice growing for half of the trayectories, and melting for the remaining ones.

Introduced in 2005 [1], the *seeding* technique's popularity has grown over the last few years being extensively applied in nucleation studies [2–16]. The *seeding* scheme can be used in two distinct ways: tracking several seeds differing in size at a given (T, P) or studying a seed with a fixed size at different (T, P). We found that the first protocol is more suitable when the critical size does not change significantly with the thermodynamic state point (i.e. $\partial N_c/\partial P \sim 0$ or $\partial N_c/\partial T \sim 0$) and we adopted it to identify N_c at most of the negative pressures. On the other hand, the second protocol (fixed seed simulated at different (T, P)) works well when the critical size is sensitive to changes of T and/or P, as observed at positive pressures, and has been adopted in this regime.

To create the initial configuration for a single *seeding* run we first equilibrate separately bulk liquid water and bulk ice at the T and P of interest. Then, we create a spherical cavity of radius R within the bulk liquid water and insert in the empty space a spherical seed of a slightly smaller radius extracted from the bulk ice. The system is quickly equilibrated at constant volume for ~ 10 ps keeping the ice-molecules motionless, which allows us to equilibrate the interface. Finally, we simulate the system in the NPT ensemble, where the pressures is applied isotropically.

In the following we show the estimation of N_c according to our *seeding* simulations.

230 K				240 K				250 K			
N_c	ΔN_c	P	Δ_P	N_c	ΔN_c	P	Δ_P	N_c	ΔN_c	P	Δ_P
3284	0	1550	50	4360	0	1050	50	5160	70	450	50
2860	300	1500	0	3560	0	1000	100	4150	70	425	25
2590	0	1450	50	2750	700	900	0	3570	500	300	0
2105	400	1400	0	2003	0	700	100	3095	70	200	100
1610	0	1300	100	1690	0	650	50	1920	50	-150	50
1022	450	900	0	1380	0	650	50	1760	50	-300	100
485	0	550	50	1520	150	600	0	1600	150	-400	0
186	25	-100	0	1085	250	500	0	1370	50	-450	150
210	25	-300	0	797	0	250	50	1280	50	-500	0
236	50	-500	0	734	105	200	0	1275	150	-600	0
225	35	-700	0	662	70	100	0	1164	60	-700	0
237	35	-900	0	582	0	1	100	1093	30	-800	0
165	55	-1300	0	531	40	-100	0	915	70	-1000	0
150	25	-1500	0	503	0	-200	100	950	50	-1300	0
189	80	-1700	0	442	70	-300	0	810	30	-1400	100
235	50	-2300	0	425	50	-500	0	802	70	-1500	0
277	50	-2700	0	432	35	-700	0	925	150	-1700	0
307	35	-3000	0	353	90	-900	0	1035	75	-1900	0
				415	30	-1100	0	1050	75	-2500	0
				393	20	-1300	0	1200	75	-2800	0
				390	45	-1500	0				
				310	45	-1700	0				
				323	35	-1900	0				
				462	55	-2300	0				
				455	80	-2500	0				
				516	35	-2700	0				
				548	40	-2900	0				

TABLE I. Seeding results. ΔN_c and Δ_P are the uncertainty of the critical nucleus size and pressure respectively.

MISLABELING CALCULATION

In Fig. 1 we report the % of mislabeled solid and liquid molecules, according to the threshold $\bar{q}_{6,t}$ of the $\bar{q}_6$ order parameter. The value of $\bar{q}_{6,t}$ is determined from the crossing of the mislabeling curves of ice and liquid water in the bulk. For any P the optimal value of $\bar{q}_{6,t}$ is well fitted by the expression $\bar{q}_{6,t}(P) = a_{q_6}(T) - b_{q_6}(T)\exp(c_{q_6}(T)P)/[d_{q_6}(T) + \exp(c_{q_6}(T)P)]$ (see Fig. 2 of SM). The fitting parameters are reported in Tab. II.

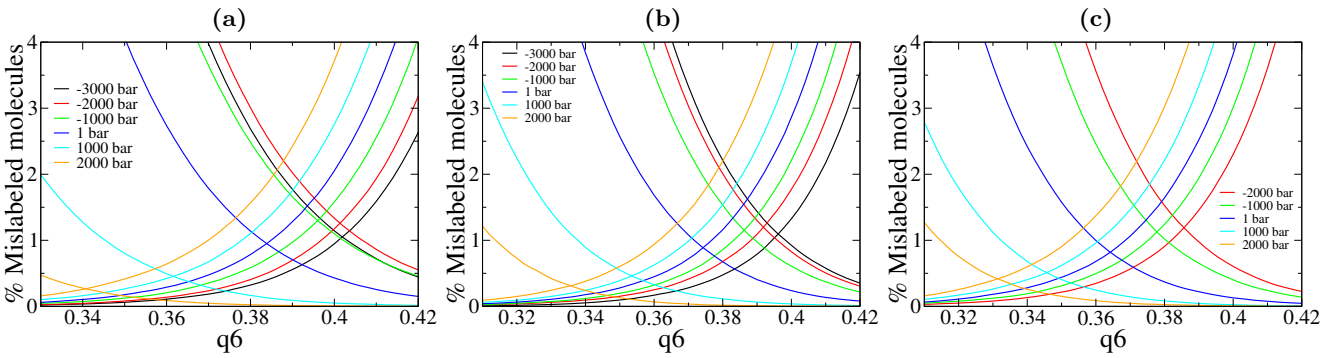

FIG. 1. Percentage of mislabeled molecules for each phase at $T = 230$ K (a), $T = 240$ K (b) and $T = 250$ K (c). Data are over equilibrium simulations of 3820 molecules in the liquid phase, and 4032 molecules in the solid Ih phase.

T [K]	$a_{q_6}(T)$	$b_{q_6}(T)$	$c_{q_6}(T)$	$d_{q_6}(T)$
230	0.401839	0.0765991	0.00127229	3.29737
240	0.396191	0.0772493	0.00106575	2.35767
250	0.392375	0.0776309	0.000938774	1.7289

TABLE II. Fitting parameters for the $\bar{q}_{6,t}$.

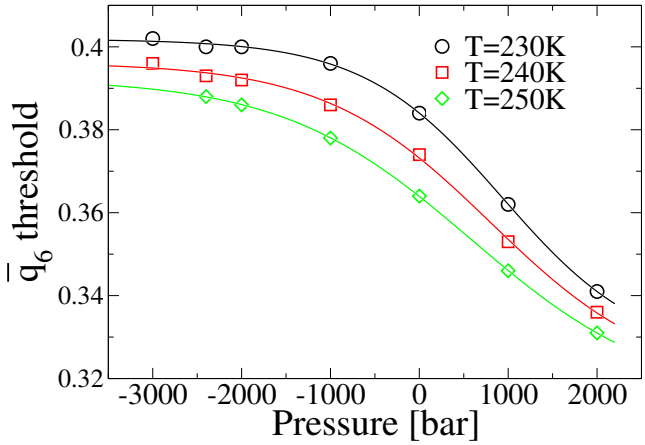

FIG. 2. Threshold $\bar{q}_{6,t}$ for the $\bar{q}_6$ order parameter as function of P, for different temperatures. Curves are fitted according to the expression reported in the SM.

CALCULATION OF $\Delta\mu$

The difference between the chemical potentials of the liquid phase μ_l and the solid phase μ_s along an isotherm, at the desired pressure P, is given by

$$\Delta\mu(P) \equiv \mu_l(P) - \mu_s(P) = \int_{P_{\rm coex}}^{P} [v_{\rm liq}^{\rm mol}(P') - v_{\rm ice}^{\rm mol}(P')]dP' \quad , \tag{1}$$

being $P_{\rm coex}$ the coexistence pressure at the temperature T, $v_{\rm liq}^{\rm mol}$ the molecular volume of the liquid phase, $v_{\rm ice}^{\rm mol}$ the molecular volume of the solid phase. The P dependence of $v_{\rm liq}^{\rm mol}$ and $v_{\rm ice}^{\rm mol}$ are shown in Fig. 3a,b. Data are fitted with $9_{\rm th}$ order polynomials, whose coefficient are reported in Tab III. It is worth noting that, along the isotherms of the liquid phase shown in Fig. 3a, the volume data cross each other at positive pressures and negative pressures. This is due to the presence of a temperature of maximum density and a temperature of minimum density, both observed upon isobaric cooling. According to our data, we have that $v_{\rm liq}^{\rm mol}(T = 240\,{\rm K}) = v_{\rm liq}^{\rm mol}(T = 250\,{\rm K})$ both at $P \sim 1500$ bar and $P \sim -2070$ bar, and $v_{\rm liq}^{\rm mol}(T = 230\,{\rm K}) = v_{\rm liq}^{\rm mol}(T = 240\,{\rm K})$ both at $P \sim 1650$ bar and $P \sim -1890$ bar. The crossing at positive pressures indicates the presence of a maximum in density, along the point $(T \sim 245\,{\rm K}, P \sim 1500\,{\rm bar})$ and $(T \sim 235\,{\rm K}, P \sim 1650\,{\rm bar})$, while the crossing at negative pressure points out the presence of a minimum in density at $(T \sim 245{\rm K}, P \sim -2070{\rm bar})$ and $(T \sim 235{\rm K}, P \sim -1890{\rm bar})$. Moreover, as shown in Fig. 3c-e, $v_{\rm liq}^{\rm mol}$ and $v_{\rm ice}^{\rm mol}$ intersects at fixed T, marking the maximum of $\Delta\mu$ shown in Fig. 5a of the main text. We found that $v_{\rm liq}^{\rm mol} = v_{\rm ice}^{\rm mol}$ at $(T = 230\,{\rm K}, P \sim -1110\,{\rm bar})$, $(T = 240\,{\rm K}, P \sim -1420\,{\rm bar})$ and $(T = 250\,{\rm K}, P \sim -1605\,{\rm bar})$.

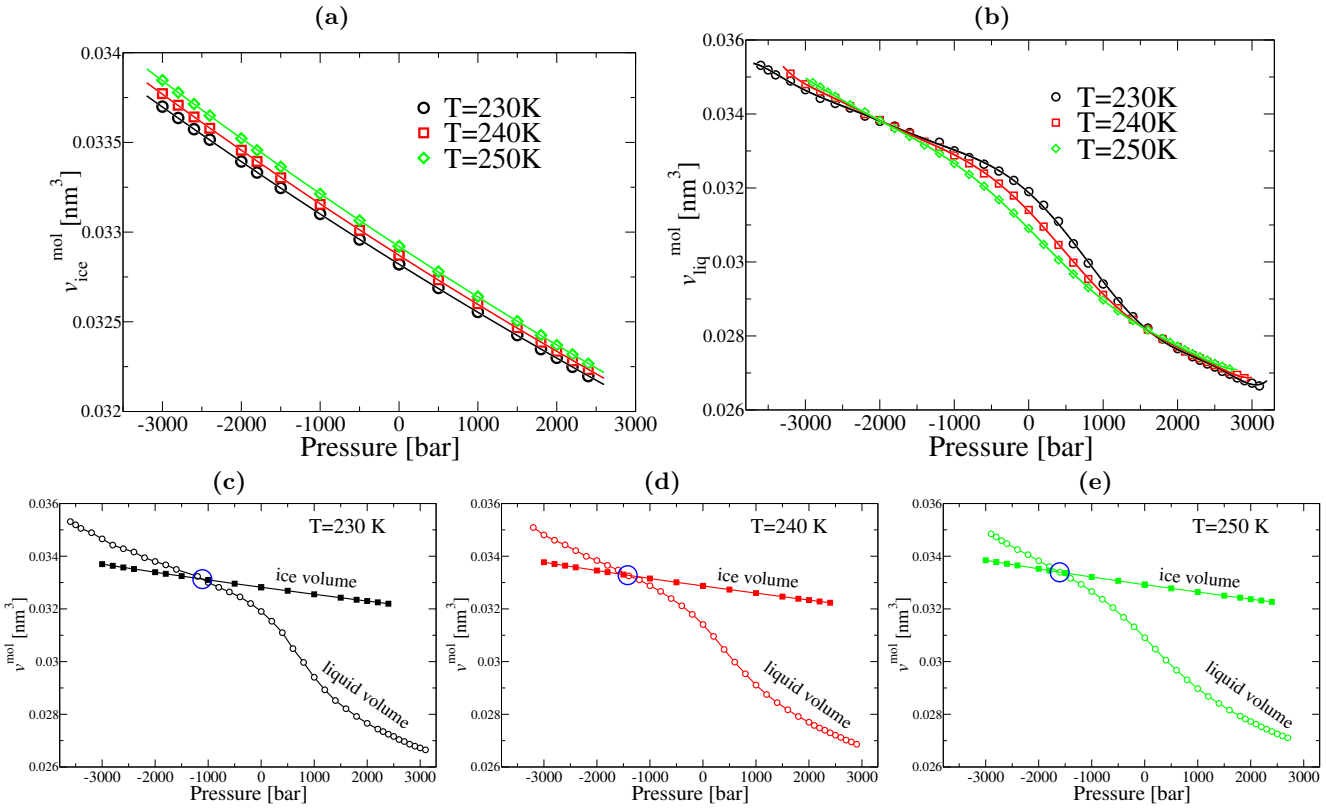

FIG. 3. Molecular volume of ice Ih $v_{\rm ice}^{mol}$ (a) and liquid water $v_{\rm liq}^{mol}$ (b) as function of pressure, for different temperatures. Data are calculated with NPT runs spanning up to 200 ns of a bulk liquid phase of 3840 molecules, and a bulk of 4032 ice molecules. Lines are polynomial fits described in the text and in TAB. III. Panels (c-e) show the molecular volume v^{mol} of liquid (open circles) and solid phase (full squares) at $T = 230$ K (c), $T = 240$ K (d) and $T = 250$ K (e). Blue circles mark the crossing between $v_{\rm ice}^{\rm mol}$ and $v_{\rm liq}^{\rm mol}$.

v	T	$a_v(T)$	$b_v(T)$	$c_v(T)$	$d_v(T)$	$e_v(T)$	$f_v(T)$	$g_v(T)$	$h_v(T)$	$i_v(T)$	$l_v(T)$
[nm^3]	[K]	($\times 10^{-34}$)	($\times 10^{-31}$)	($\times 10^{-27}$)	($\times 10^{-24}$)	($\times 10^{-20}$)	($\times 10^{-17}$)	($\times 10^{-13}$)	($\times 10^{-10}$)	($\times 10^{-6}$)	($\times 10^{-2}$)
$v_{\rm ice}^{\rm mol}$	250	0	0	0	0	0	0	0	0.0676672	-0.287745	3.29197
$v_{\rm ice}^{\rm mol}$	240	0	0	0	0	0	0	0	0.0634812	-0.280247	3.28709
$v_{\rm ice}^{\rm mol}$	230	0	0	0	0	0	0	0	0.0607871	-0.273831	3.28217
$v_{\rm liq}^{\rm mol}$	250	0	3.53928	1.56695	-5.80737	-2.9843	3.84266	2.24401	-1.1388	-2.04296	3.08979
$v_{\rm liq}^{\rm mol}$	240	0	7.91325	1.33479	-17.2535	-2.80532	13.7737	2.29159	-4.77538	-2.08529	3.13703
$v_{\rm liq}^{\rm mol}$	230	2.46393	10.0899	-5.35123	-24.2833	3.44422	21.2156	-0.0287716	-8.12152	-1.80442	3.18724

TABLE III. Coefficient of the polynomial fit for the molecular volume $v^{\rm mol}$ of liquid and solid phases, shown in Fig. 3. The fitting polynomial as function of P is $a_v(T)P^9 + b_v(T)P^8 + c_v(T)P^7 + d_v(T)P^6 + e_v(T)P^5 + f_v(T)P^4 + g_v(T)P^3 + h_v(T)P^2 + i_v(T)P + l_v(T)$.

FIT OF N_c

The pressure dependence of the ice critical size N_c has been fitted according to the expression $N_c(T,P) = a_{N_c}(T)P^2 + b_{N_c}(T)P + c_{N_c}(T) + d_{N_c}(T)\exp[e_{N_c}(T)(P + h_{N_c}(T))]$. The fitting parameters are shown in Tab. IV

T	$a_{N_c}(T)$	$b_{N_c}(T)$	$c_{N_c}(T)$	$d_{N_c}(T)$	$e_{N_c}(T)$	$h_{N_c}(T)$
[K]	($\times 10^{-4}$)		($\times 10^{2}$)		($\times 10^{-3}$)	($\times 10^{3}$)
230	0.341809	0.0797471	2.35066	0.85	2.46	1.72
240	1.32674	0.368069	5.7071	9.5	4.6	0.22
250	3.3502	1.147	18.3463	0.3	4.5	1.57

TABLE IV. Fitting parameters of the curves $N_c(T,P)$.

FIT OF D

The pressure dependence of the diffusion coefficient $D(T,P)$ is given by $D(T,P) = a_D(T) + \exp[b_D(T)P]/\{c_D(T) + d_D(T)\exp[b_D(T)P]\} + [e_D(T)P + f_D(T)P^2]/\{1 + \exp[h_D(T)P]\}$, with parameters shown in Tab. V

T	$a_D(T)$	$b_D(T)$	$c_D(T)$	$d_D(T)$	$e_D(T)$	$f_D(T)$	$h_D(T)$
[K]	($\times 10^{-4}$)	($\times 10^{-3}$)			($\times 10^{-7}$)	($\times 10^{-12}$)	($\times 10^{-3}$)
230	8.99447	3.00448	193.8014	13.68375	1.7342152	0	125.5709
240	34.87718	2.630391	28.8107	8.2971	5.737374	7.8152591	34.16511
250	311.085	2.4591358	8.3357863	7.5807725	145.64959	2217.4348	2.824802

TABLE V. Fitting parameters of the curves $D(T,P)$.

ATTACHMENT RATE f^+

The attachment rate f^+ can be rigoursly computed from the expression proposed by Auer and Frenkel[17]

$$f^+_{AF} = \frac{\langle (N(t) - N(0))^2 \rangle}{2t} \tag{2}$$

and approximated by the equation

$$f^+ = \frac{24 D N_c^{2/3}}{\lambda^2} \tag{3}$$

where D is the diffusion coefficient of the supercooled liquid, N_c the size of the critical nucleus, and $\lambda \equiv 3.8\mathring{A}$ is a characteristic length of the order of a molecular diameter [4]. In a previous work, we have applied this approximation in nucleation of ice at positive pressures finding good agreement with the rigourous procedure [4]. Here, we test it at negative pressures, also finding good agreement as can be seen in Table VI. In particular, along the 240 K isotherm, we calculate f^+ for three different negative pressures: -300 bar, -1700 bar, and -2900 bar.

P (bar)	f^+_{AF} (ns^{-1})	f^+ (ns^{-1})
-300	129.5	111.4
-1700	22.1	16.6
-2900	15.0	13.9

TABLE VI. Attachment rate computed according the rigourous Eq. 2 and approximated by the Eq. 3.

ERROR BARS FOR ΔG AND $log_{10}J$

In Fig. 4, we have a closer look at the minima of ΔG and maxima of $log_{10}J$. We also include error bars. As can be seen, the uncertainty is not enough to cover the non-monotonic behavior.

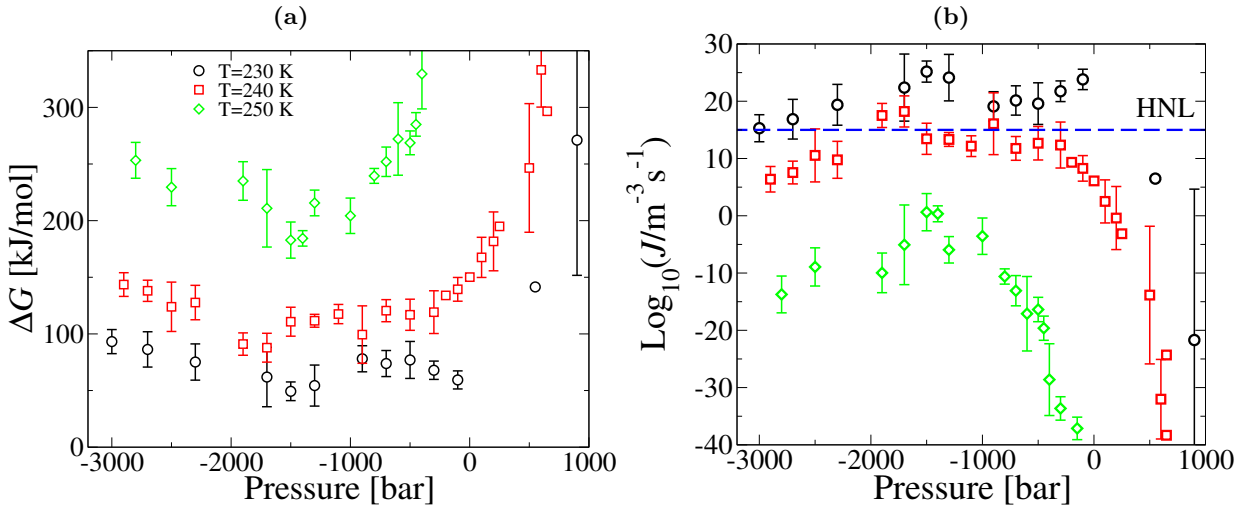

FIG. 4. Zoom in Fig. 3d) and 4b) from main text. Here, a) free energy barrier ΔG and b) the logarithm of the nucleation rate J. Error bars are included. The same legend applies in both panels.

[1] X.-M. Bai and M. Li, The Journal of Chemical Physics **122**, 224510 (2005).
[2] E. Sanz, C. Vega, J. R. Espinosa, R. Caballero-Bernal, J. L. F. Abascal, and C. Valeriani, Journal of the American Chemical Society **135**, 15008 (2013).
[3] J. R. Espinosa, C. Vega, and E. Sanz, The Journal of Physical Chemistry C **122**, 22892 (2018).
[4] J. R. Espinosa, E. Sanz, C. Valeriani, and C. Vega, The Journal of chemical physics **141**, 18C529 (2014).
[5] J. R. Espinosa, C. Vega, C. Valeriani, and E. Sanz, The Journal of Chemical Physics **144**, 034501 (2016).
[6] J. R. Espinosa, C. Navarro, E. Sanz, C. Valeriani, and C. Vega, The Journal of Chemical Physics **145**, 211922 (2016).
[7] N. E. Zimmermann, B. Vorselaars, D. Quigley, and B. Peters, Journal of the American Chemical Society **137**, 13352 (2015).
[8] B. C. Knott, V. Molinero, M. F. Doherty, and B. Peters, Journal of the American Chemical Society **134**, 19544 (2012).
[9] Y. Lifanov, B. Vorselaars, and D. Quigley, The Journal of Chemical Physics **145**, 211912 (2016).
[10] F. Leoni, R. Shi, H. Tanaka, and J. Russo, The Journal of Chemical Physics **151**, 044505 (2019).
[11] R. G. Pereyra, I. Szleifer, and M. A. Carignano, The Journal of chemical physics **135**, 034508 (2011).
[12] P. Montero de Hijes, J. R. Espinosa, E. Sanz, and C. Vega, The Journal of Chemical Physics **151**, 144501 (2019).
[13] P. Montero de Hijes, J. R. Espinosa, V. Bianco, E. Sanz, and C. Vega, The Journal of Physical Chemistry C **124**, 8795 (2020).
[14] A. O. Tipeev, E. D. Zanotto, and J. P. Rino, The Journal of Physical Chemistry C **122**, 28884 (2018).
[15] T. Dasgupta, G. M. Coli, and M. Dijkstra, ACS Nano **14**, 3957 (2020).
[16] H. Niu, L. Bonati, P. M. Piaggi, and M. Parrinello, Nature Communications **11**, 2654 (2020).
[17] S. Auer and D. Frenkel, Nature **409**, 1020 (2001).